

Embedded Knowledge Distillation in Depth-level Dynamic Neural Network

Shuchang Lyu*, Ting-Bing Xu*, and Guangliang Cheng

Abstract—In real applications, different computation-resource devices need different-depth networks (e.g., ResNet-18/34/50) with high-accuracy. Usually, existing strategies either design multiple networks (nets) and train them independently, or utilize compression techniques (e.g., low-rank decomposition, pruning, and teacher-to-student) to evolve a trained large model into a small net. These methods are subject to the low-accuracy of small nets, or complicated training processes induced by the dependence of accompanying assistive large models. In this article, we propose an elegant Depth-level Dynamic Neural Network (DDNN) integrated different-depth sub-nets of similar architectures. Instead of training individual nets with different-depth configurations, we only train a DDNN to dynamically switch different-depth sub-nets at runtime using one set of shared weight parameters. To improve the generalization of sub-nets, we design the Embedded-Knowledge-Distillation (EKD) training mechanism for the DDNN to implement semantic knowledge transfer from the teacher (full) net to multiple sub-nets. Specifically, the Kullback-Leibler divergence is introduced to constrain the posterior class probability consistency between full-net and sub-net, and self-attention on the same resolution feature of different depth is addressed to drive more abundant feature representations of sub-nets. Thus, we can obtain multiple high-accuracy sub-nets simultaneously in a DDNN via the online knowledge distillation in each training iteration without extra computation cost. Extensive experiments on CIFAR-10, CIFAR-100, and ImageNet datasets demonstrate that sub-nets in DDNN with EKD training achieves better performance than the depth-level pruning or individually training while preserving the original performance of full-net.

Index Terms—Depth-level dynamic neural network, embedded knowledge distillation, self-attention, knowledge transfer.

I. INTRODUCTION

RECENT years have witnessed significant progress in various computer vision tasks [1]–[7] using deep convolutional neural networks. To meet different resource-constrained devices, researchers usually need to design a series of different-depth networks such as VGG-13/16/19 [8], ResNet-18/34/50/101 [2], and DensNet-121/169/201 [9]. Generally, it needs to train different-depth networks individually in

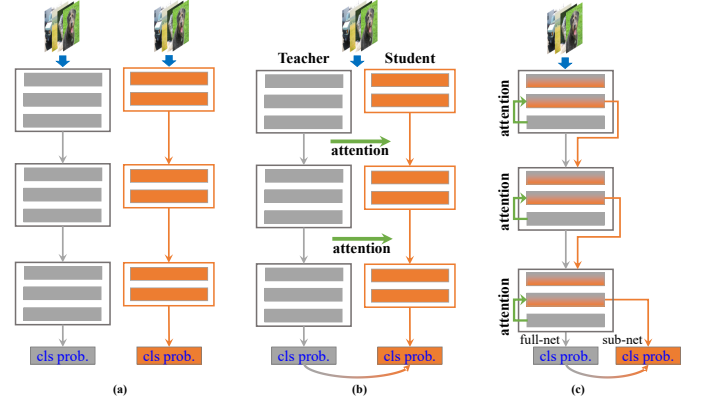


Fig. 1. Diagrams of three cases. (a) Individual multi-nets. (b) Teacher-to-student with KD. (c) DDNN with EKD.

Fig. 1(a) and download/offload different models multiple times according to device-resource constraints in real applications, which increases the training and deploying cost dramatically. In fact, the deeper ResNet-34 network (i.e., full-net) contains completely the smaller ResNet-18 architecture (i.e., sub-net) due to the configuration of the same residual structure blocks. Therefore, it motivates us to think why not directly train a single deep full-net in Fig. 1(c) to dynamically switch different-depth sub-nets during the deployment stage.

Although ResNet-50 can naturally split into different-depth sub-nets such as ResNet-41, ResNet-32, and ResNet-26 using only a set of the shared weight parameters, a key problem is how to train the four networks (i.e., one full-net and three sub-nets) simultaneously in one depth-level dynamic neural network (DDNN) while preserving high accuracy. The naive strategy is that we only train one single deep full-net and directly use multiple sub-nets during the test stage. However, these sub-nets are easily subjected to the worse generalization ability due to the lacking of training on respective optimization objective. Another strategy is that we train the DDNN with multiple optimization objectives from different-depth networks. Nevertheless, those layers of shared weights are very hard to simultaneously match the different objectives, which will lead to lower accuracy than independently training the multiple sub-nets without shared weights. Thus, we need to design a more reasonable training mechanism for the DDNN to improve the performance of sub-nets while preserving the original accuracy of full-net.

How to obtain a small yet high-accuracy network has also been widely studied in network compression and acceleration field. They mainly adopt network compression techniques such

*indicates equal contribution. This work was supported in part by the Natural Science Foundation of Beijing, China under Grant 4214074. (Corresponding author: Ting-Bing Xu.)

Shuchang Lyu is with the School of Electronic and Information Engineering, Beihang University, Beijing 100191, China (e-mail: lyushuchang@buaa.edu.cn).

Ting-Bing Xu is with the Key Laboratory of Precision Opto-mechatronics Technology, Ministry of Education, Beihang University, Beijing 100191, China, and also with the School of Instrumentation Science and Opto-electronics Engineering, Beihang University, Beijing 100191, China (e-mail: tingbing_xu@buaa.edu.cn).

Guangliang Cheng is with the SenseTime Research, Beijing 100080, China (e-mail: guangliangcheng2014@gmail.com).

as matrix decomposition, weight or channel pruning, quantization, and knowledge distillation to evolve a large trained model into a small network without accuracy loss. Especially, Huang et al. [10] have extended channel-level pruning to depth-level pruning that can dynamically remove the whole residual block using the sparse scaling factor. Similarly, BlockDrop [11] and SkipNet [12] also introduce different dynamic inference path selection strategies to implement the depth-level pruning. Despite their effective improvement of final small network performance, they cannot obtain multiple high-accuracy small networks simultaneously.

To effectively train one DDNN with multiple sub-nets, we review the common two-step knowledge distillation in Fig. 1(b). A deep yet complex teacher network is trained first, and then the small student network is trained with extra supervised information (e.g., class probabilities [13], logits [14], intermediate feature map [15], and attention map [16]) of teacher model to inherit the dark knowledge (i.e., powerful representative ability). Inspired by this, we design the Embedded-Knowledge-Distillation (EKD) training mechanism in Fig. 1(c) to substantially improve the performance of multiple sub-nets in one DDNN. Specifically, we utilize the predicted class posterior probabilities of full-net as soft labels to construct Kullback-Leibler (KL) divergence constraint for guiding the learning of different-depth sub-nets, and introduce the self-attention on the same resolution feature of different-depth to drive the learned semantic feature as consistency as possible between full-net and sub-net. Meanwhile, we still keep the conventional cross-entropy loss term (i.e., softmax loss) with hard labels for the training of full-net and sub-nets. The abovementioned three types of loss terms can be integrated together as the optimization objective to fulfil the EKD learning of DDNN from scratch in an end-to-end manner. Thus, the EKD training mechanism can naturally implement the online knowledge distillation of DDNN in each training iteration without additional computation and memory cost.

To verify the effectiveness of proposed method, we conduct extensive experiments on multiple benchmark datasets (e.g., CIFAR-10 [17], CIFAR-100 [17], and ImageNet [18]) with current state-of-the-art networks (e.g., VGGNet [8], ResNet [2]). Compared to the depth-level pruning and individually training strategies without shared weights, sub-nets in DDNN with EKD training achieves higher performance while preserving the original accuracy of full-net.

The main contributions can be summarized as follows.

- 1) One Depth-level Dynamic Neural Network is proposed, which can simultaneously extract multiple different-depth sub-nets in a full-net for satisfying the requirement of different resource-constrained devices.
- 2) Embedded-Knowledge-Distillation training mechanism is designed to effectively improve the representative capacity of multiple sub-nets in a DDNN with the inner self-supervision manner.
- 3) Sub-nets with EKD training achieve a considerable performance improvement, especially for small sub-nets, which improve $\sim 1\%$ than individual training strategy on CIFAR and ImageNet.

- 4) Sub-nets in a DDNN could achieve better accuracy than the depth-level pruning networks of the equivalent number of weight parameters and FLOPs¹.

The remainder of this article is organized as follows. Section II reviews related works; Section III describes the details of the proposed method; Section IV presents experimental results and discussions, and Section V draws concluding remarks.

II. RELATED WORK

A. High-efficiency Network

In recent years, researchers have designed many network compression and acceleration methods to harvest the high-performance small networks, i.e., the high-efficiency networks for embedded devices with limited computing resource. For example, some compact units such as Fire module [19], Inception module [20], Residual block [2], and Depthwise [21], have been exploited to construct respective compact network architectures like SqueezeNet [19], InceptionNet [22], ResNet [2], MobileNet [23], ShuffleNet [24], etc. To achieve a larger parameter compression, a series of low-bit quantization methods [25]–[28] have also been proposed to compress and accelerate baseline models dramatically. Especially, the extremely binarized networks such as BinaryConnect [29], BinarizedNet [25], and XNOR-Net [26] use only 1-bit (± 1) type to represent weight parameter and feature map response, which can save model storage by $32\times$ and accelerate inference time by using the simple 1-bit XNOR and bitcounting operations instead of the complex floating point multiply-accumulate operations. Nevertheless, deep binarized networks are easily subjected to the severe performance drop.

To reduce parameter redundancies, a series of tangible network pruning methods such as the low-threshold pruning of non-structured sparsity [30]–[32] and the structured pruning [33]–[35] have been designed to find a more efficient sub-net from a trained large model while preserving the performance of large model. Although these approaches obtain a high-performance small model, they usually require a pre-trained model and involve a very costly and tricky training process, including careful hyper-parameter setting, iterative pruning, and fine-tuning after each pruning step. our DDNN with EKD training can also be viewed as a type of depth-level pruning without the requirement of a complex training process. Once the sub-net achieves similar performance as the full-net, the remaining redundant layers of the full-net can be pruned directly without incurring the severe performance drop.

B. Knowledge distillation

Instead of the high-efficiency sub-net architecture search in network pruning, knowledge distillation [13] exploits the potential capacity of fixed sub-net by knowledge transfer from a larger teacher model to a small student network. It is now widely used in various computer vision tasks such as classification [13]–[16], [36], detection [37], [38], segmentation [39], [40], and re-identification [41], which effectively improves the performance of small student model by taking the extra

¹FLOPs: FLoating-point OPerations

supervised information of a pre-trained teacher model. Trained in this manner, the student network inherits the teacher's properties, such as the final class probabilities, logits, and the intermediate feature maps, which can be taken as the soft-targets to guide student network for better learning. Although their success in improving the performance of the small model, the accompanying training mechanism of cumbersome pre-trained teacher model (maybe an ensemble of multiple models) complicates training process and increases memory/time cost. Also, teacher-to-student training cannot obtain multiple high-efficiency small networks simultaneously, i.e., only one high-performance small model at one time and the small network architecture is also fixed, which lacks the flexibility and extendibility.

C. Dynamic Neural Network

Dynamic neural network aims at extracting the different-depth or different-width sub-net dynamically from a deep network according to the configuration of computation and memory budgets. BlockDrop [11] proposes the depth-level layer choice approach to dynamically drop some useless residual blocks of ResNet on-the-fly so as to best reduce total computation without degrading prediction accuracy. SkipNet [12] uses the gating policy network to selectively skip some unnecessary residual blocks and incorporates reinforcement learning into the supervised problem to implement the non-differentiable skipping decisions. Similarly, Dynamic deep neural network [42] adopt the directed acyclic graph of differentiable modules to fulfil the dynamic selective execution, where only the subset neurons of full-net are executed for a given input.

Recently, dynamic neural network has been extended to switch multiple sub-nets simultaneously from a deep network, which can maximally re-use parameters and computation each other. Huang et al. [43] exploit multi-scale dense networks to automatically switch different resource-efficient sub-nets for each specific test example, i.e., small networks for the easy test sample and big networks for the hard test sample. Yu et al. [44] design slimmable neural networks to address a key question "Given budgets of resources, how to instantly, adaptively and efficiently trade-off between accuracy and latency for neural networks at runtime?", which only train a shared network with switchable batch normalization to adjust its width on-the-fly for the constructions of different-width sub-nets. In [45], they integrated further sandwich rule and inplace distillation into slimmable networks to enhance the training process and boost test accuracies of full-net and sub-nets.

III. METHODOLOGY

Dynamic neural network can be designed from the width-level and depth-level perspectives. In this article, we mainly focus on constructing depth-level dynamic neural network (DDNN) integrated multiple sub-nets with the shared weight parameters and exploiting the Embedded-Knowledge-Distillation (EKD) training mechanism to excavate the potential representative capacity of multiple sub-nets in one DDNN without additional computation and storage cost.

A. Depth-level Dynamic Neural Network

Depth-level dynamic neural network denotes that one deep neural network (i.e., full-net) can dynamically switch its depth on-the-fly to yield different-depth sub-nets for different resource-limited devices. The specific formulation can be written as

$$A_{\text{sub-net}_k} = \text{Switch}_{\text{depth}}(A_{\text{full-net}}), \quad k = 1, \dots, K \quad (1)$$

where A represents the architecture of the network and K is the total number of sub-nets from one full-net.

Usually, we select a large baseline network as the full-net to design the depth-level dynamic neural network. We first separate the large baseline network into several stages according to the resolution of output feature maps. Then, we skip the deep blocks of some stages to create sub-stage. Finally, a sub-net is formed by creating directly connections between sub-stages of each two neighbouring stage. Here, we select the standard ResNet-50 [2] architecture as an example in Fig. 2 to introduce our construction of DDNN. In this case, the baseline ResNet-50 network is the full-net containing four stages (i.e., Full-net [3 4 6 3]), each of which contains 3/4/6/3 residual bottleneck blocks respectively. The residual bottleneck blocks in the middle two stages are split into different parts. We then create skip connections to make output features of sub-nets (orange line and red line in Fig. 2) directly jump to the next stage. When stitching the corresponding classifiers for sub-nets in the end, the DDNN including ResNet-50, ResNet-44 (i.e., Sub-net2 [3 4 4 3]) and ResNet-38 (i.e., Sub-net1 [3 3 3 3]) would be formed. Besides, our proposed DDNN can also contain the different number of sub-nets depending on practical demand.

B. Embedded Knowledge Distillation

Dynamic Neural Network can be trained in an end-to-end manner through optimizing full-net and sub-nets with only hard labels. However, because of the weight-sharing case, some shared residual blocks in different networks are forced to represent different semantic feature patterns. It will result in the performance decline of both full-net and sub-nets than networks independently trained without the sharing case. To address this problem, we design the embedded-knowledge-distillation (EKD) training mechanism to excavate the potential representative capacity of the proposed DDNN for higher parameter efficiency.

Fig. 2 shows the detailed training process of our DDNN with the EKD training mechanism. The full-net [3 4 6 3] is used as "teacher model" to provide extra supervised information (i.e., soft labels in Fig. 2) for guiding the better learning of sub-nets (i.e., student models). Meanwhile, the full-net also benefits from better sub-nets because of possessing better sub-nets as "backbone". Besides, full-net and sub-nets are also all optimized with hard labels. Moreover, the self-attention module is introduced to constrain the predicted semantic feature consistency between full-net and sub-nets.

1) *Distillation on posterior class probabilities*: Generally, we use the softmax operation to yield the posterior class

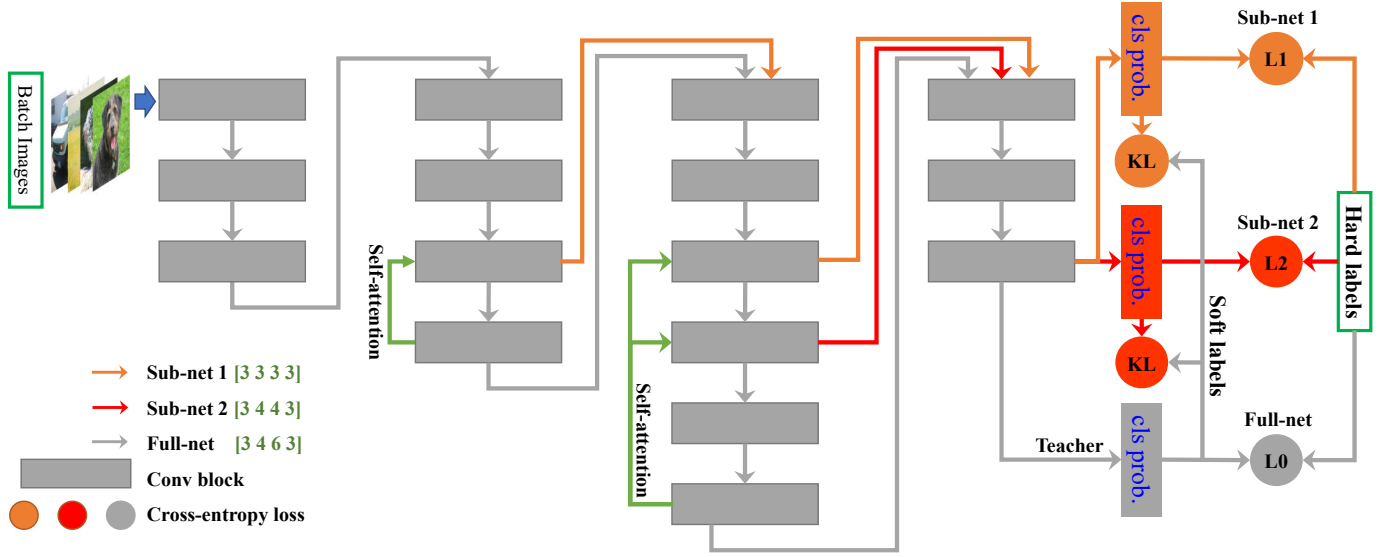


Fig. 2. Proposed depth-level dynamic neural network with embedded knowledge distillation training. “Conv block” denotes one residual bottleneck block. Full-net is ResNet-50 while sub-nets are ResNet-44 and ResNet-38. [3, 4, 6, 3] means each stage of full-net contain 3, 4, 6 and 3 residual blocks respectively.

probability $p(\hat{y} = y_m | \mathbf{x})$ for each input sample \mathbf{x} ². The specific formulation can be written as

$$p(\hat{y} = y_m | \mathbf{x}) = \text{softmax}(z_m) = \frac{e^{z_m}}{\sum_{j=1}^M e^{z_j}} \quad (2)$$

where it denotes the predicted probability of \mathbf{x} from class y_m and z represents the logit, i.e., the output of the last fully-connected linear classifier layer. M is total number of classes. Then, we can denote the predicted posterior probability vector of full-net (i.e., teacher in Fig. 2) as $\mathbf{p}_t(\mathbf{x}) = \{p_t(\hat{y} = 1 | \mathbf{x}), \dots, p_t(\hat{y} = M | \mathbf{x})\}$. Similarly, the predicted posterior probability vector of each sub-net is defined as

$$\mathbf{p}_s^k(\mathbf{x}) = \{p_s(\hat{y} = 1 | \mathbf{x}), \dots, p_s(\hat{y} = M | \mathbf{x})\}, \quad k = 1, \dots, K \quad (3)$$

where K represents the total number of sub-nets in one full-net. Thus, we can easily implement the online knowledge distillation from full-net to sub-net in each training step. The \mathbf{p}_t can be viewed as the extra supervised information (i.e., soft label in Fig. 2) from full-net to guide the learning of sub-net. Here, we use the common Kullback-Leibler divergence constraint as distillation loss, its formulation is defined as

$$\begin{aligned} KL_s^k &= \frac{1}{n} \sum_{n=1}^N KL(\mathbf{p}_t(\mathbf{x}_n) \| \mathbf{p}_s^k(\mathbf{x}_n)) \\ &= -\frac{1}{n} \sum_{n=1}^N \mathbf{p}_t(\mathbf{x}_n) \log \frac{\mathbf{p}_s^k(\mathbf{x}_n)}{\mathbf{p}_t(\mathbf{x}_n)} \end{aligned} \quad (4)$$

where it denotes the KL distance from \mathbf{p}_s^k to \mathbf{p}_t and N is the number of samples in a mini-batch. The soft label \mathbf{p}_t is different from the regular hard label (i.e., one-hot vector $0, \dots, 1, 0$). One-hot objective lacks the inter-class relation. In contrast, the soft label from full-net (teacher) possesses the richer inter-class information, such as the predicted probability

²Bold indicates a vector or a matrix.

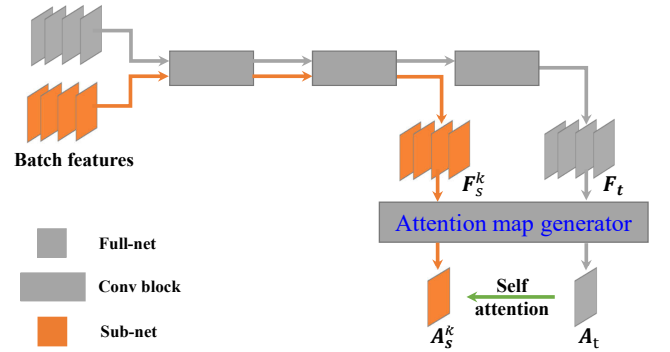


Fig. 3. Self-attention on feature maps. Attention map generator is used for both sub-nets and full-net to create attention map from feature maps.

vector of a “car” image is more proximate to a “truck” image than to a “cat” image, which is more similar to the human visual system. Meanwhile, the guided learning of soft labels also effectively prevents the overconfidence of the predicted probability on the single class. Trained in this way, the sub-net can inherit the more powerful capacity of posterior probability prediction from the full-net.

2) *Self-attention on feature maps*: To further make the semantic feature in the same stage as consistent as possible between full-net and sub-net, we introduce the self-attention module shown in Fig. 3. We respectively denote the feature maps of full-net and sub-nets as F_t and F_s^k ($F_t, F_s^k \in \mathbb{R}^{C \times H \times W}$), where C denotes the total number of channels. At the same resolution stage, these feature maps are first fed into the attention map generator to create the corresponding semantic attention map ($A_t, A_s^k \in \mathbb{R}^{1 \times H \times W}$) through calculating the element-wise sum of all absolute values across channels. Here, F_s^k and A_s^k represents feature maps and the semantic attention map of the k^{th} sub-net respectively. The specific formulation

can be written as

$$A_t = \sum_{c=1}^C |(F_t)_c|, \quad A_s^k = \sum_{c=1}^C |(F_s^k)_c| \quad (5)$$

Note that the A_t in full-net and A_s^k in sub-net are from the same resolution stage while possessing different semantic features due to the source of different-depth layers in the same DDNN, i.e., the green line in Fig. 2. Thus, the semantic attention map A_t from the deeper layer can guide the learning of A_s^k via the self-attention constraint. Here, we adopt mean-squared-error (MSE) loss to implement the online self-attention learning in each training step, it can be denoted as

$$\begin{aligned} MSE_s^k &= \frac{1}{n} \sum_{n=1}^N MSE(A_s^k(\mathbf{x}_n) \| A_t(\mathbf{x}_n)) \\ &= \frac{1}{n} \sum_{n=1}^N \sum_{h=1}^H \sum_{w=1}^W ((a_s^k(\mathbf{x}_n))_{hw} - (a_t(\mathbf{x}_n))_{hw})^2 \end{aligned} \quad (6)$$

where H, W are the height and width of the attention map respectively, and $(a_s^k)_{hw}$ denotes the value at position (h, w) of attention map from the k^{th} sub-net. Thus, the attention map A_t of full-net can be viewed as the teacher drives the attention map A_s^k of each sub-net to learn more powerful semantic feature representations, which can effectively improve their performance.

C. Optimization

Our DDNN fulfils the online EKD learning via the above-mentioned two types of loss terms (i.e., KL and MSE). Except for them, the full-net and sub-nets in one DDNN still require possessing the capacity of predicting correct classes, therefore we keep the conventional softmax cross-entropy loss term with hard label for each network in DDNN (the right side in Fig. 2). For each network, this term is defined as

$$L_k = -\frac{1}{n} \sum_{n=1}^N \log p(\hat{y} = y_n | \mathbf{x}_n) \quad (7)$$

where (\mathbf{x}_n, y_n) represents the input and hard label of current sample, and $p(\hat{y} = y_n | \mathbf{x}_n)$ is the posterior class probability of predicting correct label. Thus, the optimization objective of each sub-net consist of KL_s^k , MSE_s^k , and L_k , where k denotes the k^{th} sub-net. Finally, we can integrate the formula (4), (6), and (7) to construct the whole objective of DDNN with EKD training, the total loss is defined as

$$\begin{aligned} L_{DDNN} &= L_{full-net} + L_{sub-net \ 1} + \dots + L_{sub-net \ K} \\ &= L_0 + \underbrace{\frac{1}{K} \sum_{k=1}^K L_k}_{\text{softmax cross-entropy loss}} \\ &\quad + \underbrace{\frac{1}{K} \sum_{k=1}^K w_k \cdot KL(\mathbf{p}_t \| \mathbf{p}_s^k)}_{\text{KL distillation loss}} \\ &\quad + \underbrace{\frac{1}{K} \sum_{k=1}^K \alpha_k \cdot MSE(A_s^k \| A_t)}_{\text{Self-attention loss}} \end{aligned} \quad (8)$$

where w_k and α_k are the hyper-parameters to adjust the proportions of KL distillation loss and MSE self-attention loss respectively. For different tasks, we adopt different hyper-parameter strategies to make DDNN training work well. On the CIFAR-10 task, we increase the training intensity of KL_s^k because the total number of classes is only 10, which is easy for sub-nets to learn the pattern of full-net's predicted class probability. On the CIFAR-100 and ImageNet tasks, due to the final class probability is more complex, we appropriately increase the proportion of self-attention loss to help sub-nets learn semantic features from full-net.

From an architecture design perspective, our DDNN can keep the flexibility by dynamically switching the different-depth sub-nets at runtime. From the learning manner, the EKD training mechanism can achieve better results on both sub-nets and full-net, which indicates that full-net can also more or less benefits from better sub-nets in some cases. Compared with full-net, some sub-nets can achieve very similar or even better results. In this case, we can directly prune the redundant layers of full-net, i.e., compress the model without any fine-tuning. Meanwhile, we compare the performance of our sub-nets with notable compression models [10], [46] and get competitive results.

The proposed DDNN with EKD training process can be implemented in an end-to-end manner and optimized via the layer-wise gradient backpropagation in Algorithm 1.

Algorithm 1 DDNN with EKD training.

► Training

Input: A minibatch of training samples $B = \{(\mathbf{x}_1, y_1), \dots, (\mathbf{x}_N, y_N)\}$. Define the architecture of DDNN and the split point in different stages (stage num: η) to create K sub-nets. For example, ResNet-50/44/38 in Fig. 2, $\eta = 2$, $K = 2$.

Initialize weight parameters $\mathbf{W} = \{\mathbf{W}_1, \dots, \mathbf{W}_l\}$.

Output: updated parameters $\mathbf{W} = \{\mathbf{W}_1, \dots, \mathbf{W}_l\}$.

Forward Propagation:

$\mathbf{h}(0) = B \in \mathbb{R}^{N \times C \times H \times W}$

Clear weight gradients with *zero-grad* operation

for $q = 1$ to l layers **do**

 Compute the feature representation of each layer:

$\mathbf{h}(q) = f(\mathbf{W}_q \cdot \mathbf{h}(q-1))$

end for

Get posterior class probability with *softmax* operation

Compute cross-entropy loss: $L_k(\hat{y}, y)$ by using (7)

Compute distillation loss: $KL(\mathbf{p}_t \| \mathbf{p}_s^k)$ by using (4)

Get attention map: A_t and A_s^k by using (5)

Compute attention loss: $MSE(A_s^k \| A_t)$ by using (6)

Backward Propagation:

Update the \mathbf{W}_l with the joint loss: L_k and KL

Gather weight gradients with total loss: L_{DDNN} in (8)

for $q = l-1$ to 1 layers **do**

 Compute weight gradients with *backward* operation

 Update weights \mathbf{W}_q with *step* operation

end for

TABLE I
STRUCTURE CONFIGURATION OF VARIOUS MODELS

CIFAR		ImageNet	
Networks	Structure	Networks	Structure
ResNet-16	[3, 2, 2]	ResNet-18	[2, 2, 2, 2]
ResNet-20	[3, 3, 3]	ResNet-34	[3, 4, 6, 3]
ResNet-32	[5, 5, 5]	ResNet-26 (C)	[2, 2, 2, 2]
ResNet-44	[7, 7, 7]	ResNet-32 (C)	[2, 3, 3, 2]
ResNet-56	[9, 9, 9]	ResNet-38 (C)	[3, 3, 3, 3]
VGG-11	[1, 1, 2, 2, 2]	ResNet-41 (C)	[3, 4, 4, 2]
VGG-13	[2, 2, 2, 2, 2]	ResNet-44 (C)	[3, 4, 4, 3]
VGG-16	[2, 2, 3, 3, 3]	ResNet-50 (C)	[3, 4, 6, 3]

IV. EXPERIMENTS

To evaluate our proposed method, we conduct extensive experiments and exhaustive comparisons on CIFAR-10, CIFAR-100, and ImageNet benchmark datasets. Experimental results demonstrate that the EKD training mechanism can better explore the potential capacity of sub-nets in DDNN. Experiments also show that sub-nets in DDNN can outperform state-of-the-art depth-level pruning models. All the experiments were performed with the PyTorch [47] platform.

A. Datasets and Implementation Details

In this article, the used datasets are described as follows. We evaluate our method on CIFAR³ databases [17]. The **CIFAR-10** is an established computer-vision dataset used for object recognition, which consists of 32×32 color natural images in 10 object classes containing 50,000 training images (5000 samples per class) and 10,000 test images (1000 samples per class). The **CIFAR-100** is a more challenging object recognition dataset, which consists of 32×32 color images in 100 object classes containing 50,000 training images (only 500 samples per class) and 10,000 test images (only 100 samples per class). All the images are preprocessed by using the simple channel means and standard deviations while adopting the regular data-augmentation strategy during the training stage that has been widely used: training images are padded four pixels with zero-value on each side and randomly crop a 32×32 region from the padded image or its mirror flip. In addition, we also conduct the related experiments on the **ImageNet**⁴ Large Scale Visual Recognition Challenge (ILSVRC) dataset [18], which contains about 1.28 million training images and 50,000 validation images from 1000 classes. All the raw images are from the different-resolution high-quality color image, where the height or width of the image can be from about 100 pixels to more than 1000 pixels. For the data augmentation, we adopt the scale and aspect ratio augmentation from [48], i.e., randomly cropping a various sized patch of the raw image whose size is distributed between 8% and 100% of the image and whose aspect ratio is chosen randomly between 3/4 and 4/3, then the patch is resized to 224×224 and randomly

TABLE II
TOP-1 ERROR RATE (%) ON CIFAR-10 AND CIFAR-100

Networks	CIFAR-10			CIFAR-100		
	Individual	DDNN	EKD	Individual	DDNN	EKD
ResNet-16 (sub)	8.87	8.91	8.13	33.95	34.23	32.65
ResNet-20 (full)	7.92	8.31	8.00	32.52	33.11	32.21
ResNet-20 (sub)	7.92	8.00	7.49	32.52	32.62	31.31
ResNet-32 (full)	7.25	7.72	7.34	30.10	31.75	30.95
ResNet-32 (sub)	7.25	7.15	6.75	30.10	29.97	29.57
ResNet-44 (full)	6.49	6.78	6.60	29.23	29.81	29.51
ResNet-44 (sub)	6.49	6.77	6.05	29.23	29.16	28.36
ResNet-56 (full)	6.09	6.24	6.11	28.58	28.76	28.38
ResNet-32 (sub)	7.25	7.57	6.98	30.10	31.40	29.49
ResNet-44 (sub)	6.49	6.62	6.24	29.23	29.88	29.02
ResNet-56 (full)	6.09	6.39	6.17	28.58	29.02	28.81
VGG-11 (sub)	7.68	7.75	7.05	32.00	31.73	30.94
VGG-16 (full)	6.19	6.42	6.34	27.72	28.42	27.93
VGG-13 (sub)	6.23	6.26	6.24	28.55	28.65	28.23
VGG-16 (full)	6.09	6.08	6.14	27.72	27.64	27.81

does the mirror flip operation. Note that we only apply the single-crop operation of the central region at test time.

For implementation details, we mainly use ResNets [2], [49] and VGG [8] as full-nets to construct the DDNN architecture. Specially, we follow the specific implementation of baseline full-net in [50]. To make a fair comparison, we give out fixed training settings for each benchmark. On CIFAR, we use stochastic gradient descent (SGD) with the momentum of 0.9 and weight decay of 0.0001. The initial learning rate is set to 0.1 and the mini-batch size is set to 128. The total number of training epochs is 300 and the learning rate will be divided by 10 at epoch 150 and 250. On ImageNet, we follow the optimizer settings of CIAFR. Differently, every network is trained for 110 epochs. The learning rate is set to 0.1 initially and decreases by 10 times at epoch 30, 60, and 90.

To clearly show the structure configuration of our models, Table I gives out the number of building blocks in each model. If the baseline model belongs to ResNet series [2], the building block can be the basic residual block or residual bottleneck block depending on the original design of the respective baseline. Specifically, the building blocks on the CIFAR task are all the basic residual blocks, meanwhile, the configuration of residual bottleneck block on the ImageNet task has been marked by “C” in the bracket. If the baseline model belongs to VGG [8] series, the building block is the basic structure like “[Conv-BN-ReLU]”, and various VGG models have the same basic structure design (except for the classifier) on CIFAR and ImageNet tasks. Table I displays the detailed settings. Other detailed settings will be kept the same as previous works.

B. Experimental Results

1) *CIFAR-10/100 Object Recognition*: We first design the DDNN architecture based on baseline models of ResNet [2] and VGG [8]. Then we incorporate the EKD training mechanism into the DDNN and calculate the top-1 classification error of each sub-net respectively. Table II gives the detailed comparisons of three cases: training full-net and sub-nets individually without weight sharing in Fig. 1(a), training one DDNN integrated full-net and sub-nets with weight sharing,

³Data are available at <http://www.cs.toronto.edu/~kriz/cifar.html>

⁴Data are available at <http://www.image-net.org/challenges/LSVRC/>

TABLE III
TOP-1 ERROR RATE (%) ON IMAGENET

Individual networks			DDNN trained with only hard labels			DDNN trained with EKD mechanism			FLOPs
Networks	Params	Top-1 Err.	Networks	Params	Top-1 Err.	Networks	Params	Top-1 Err.	
ResNet-18	11.7M	31.22	D-ResNet-34-18	21.8M	30.96	EKD-ResNet-34-18	21.8M	30.24	1.8G
ResNet-34	21.8M	26.73	(full: res-34, sub: res18)		27.44	(full: res34, sub: res18)		27.02	3.6G
ResNet-26	16.0M	27.56	D-ResNet-50-26	25.6M	28.22	EKD-ResNet-50-26	25.6M	27.01	2.3G
ResNet-50	25.6M	23.94	(full: res50, sub: res26)		25.14	(full: res50, sub: res26)		24.44	3.8G
ResNet-32	17.4M	26.13	D-ResNet-50-32	25.6M	27.03	EKD-ResNet-50-32	25.6M	25.66	2.8G
ResNet-50	25.6M	23.94	(full: res50, sub: res32)		24.86	(full: res50, sub: res32)		24.06	3.8G
ResNet-41	18.9M	24.80	D-ResNet-50-41	25.6M	25.71	EKD-ResNet-50-41	25.6M	24.24	3.4G
ResNet-50	25.6M	23.94	(full: res50, sub: res41)		24.69	(full: res50, sub: res41)		23.89	3.8G
ResNet-38	21.9M	25.19	D-ResNet-50-44-38	25.6M	26.45	EKD-ResNet-50-44-38	25.6M	24.83	3.2G
ResNet-44	23.3M	24.68	(sub2: res44, sub1: res38)		25.32	(sub2: res44, sub1: res38)		24.35	3.7G
ResNet-50	25.6M	23.94	(full: res50)		25.03	(full: res50)		24.02	3.8G

and training the DDNN with the proposed EKD mechanism. As described in Section III-B, the DDNN trained with only the optimization objective of hard labels from full-net and sub-nets (2nd column) has lower performance than independently trained full-net and sub-nets without weight sharing (1st column), which mainly reason is that these layers of shared weights are very hard to simultaneously match the multiple different optimization objectives from full-net and sub-nets. To improve the training of full-net and sub-nets in one DDNN, we design a more reasonable EKD training mechanism. Experimental results on the CIFAR-10 show that sub-nets in DDNN with EKD training (3rd column) possess the average 1~2% improvement compared to sub-nets in DDNN with the only hard labels (2nd column). Even compared with the independently trained case (1st column), sub-nets in DDNN with EKD training still have the 0.5~1% lower error rate (Bold in Table II) while preserving the little performance decline of full-net. Especially, when the sub-net (ResNet-44) and full-net (ResNet-56) are both have strong and closed performance, it can achieve the inspiring effect by mixing them into one DDNN with EKD training.

Similarly, the experimental results of CIFAR-100 in Table II also show that the models with EKD training perform far better than DDNN with the only hard labels, meanwhile, sub-nets in DDNN with EKD training can obviously surpass the independently trained case. Especially, the relatively smaller sub-net, like ResNet-16 and ResNet-20, can achieve the $> 1\%$ (33.95%~32.65%) improvement than the independently trained baselines. It further indicates that smaller models possess a great room for improvement, meanwhile, our proposed EKD mechanism can maximally exploit the potential representative capacity of them.

From Table II, we can also know that the DDNN on CIFAR-100 has more obvious performance decline than on CIFAR-10 when it does not use the EKD training mechanism. This demonstrates that increasing the complexity of the task (e.g., CIFAR-100 has 100 classes and only 500 training samples per class) would incur a more big performance drop, i.e., these layers of shared weights in the complex task are more harder to simultaneously match the different objectives for the DDNN trained with the only hard labels. Furthermore, our EKD can

effectively remove this kind of performance decline, which fully displays the effectiveness of the proposed mechanism.

2) *Large-Scale ImageNet Visual Recognition*: To further verify the effectiveness of the proposed EKD training mechanism, we also conduct extensive experiments on the large-scale ImageNet visual recognition challenge task where total categories are 1000 classes and total training samples are 1.28 million training images (~1000 images per class).

Table III gives detailed comparisons of three different training frameworks in terms of network architecture, network parameters, and top-1 error rate. As expected, our DDNN can integrate multiple networks (i.e., full-net and multiple sub-nets) into one network from architecture-design respective. Thus, we only require the weight parameters of one full-net to implement the training of multiple networks in DDNN and can dynamically switch the depth of DDNN during the test stage to fulfil the deployment of different-depth sub-nets for different resource-limited devices. Although the DDNN can dramatically reduce the network parameters, full-net and sub-nets in DDNN trained with only hard labels incur obvious performance decline. Especially, full-net (i.e., full in Table III) increases the top-1 error rate by about 1%.

To address the shortage, we design the dedicated EKD training mechanism for the proposed DDNN. From the results in Table III, we can see that the EKD mechanism can obviously improve the performance decline of full-net and sub-nets in DDNN. Sub-nets in DDNN with EKD training mechanism can achieve the $> 1\%$ improvement than that without EKD mechanism. Especially, EKD possesses more excellent capacity for improving the performance of smaller sub-nets. Even, sub-nets in DDNN with EKD can surpass the baseline of the independently trained case by 0.5~1% (Bold in Table III), for example, decreasing the error rate of ResNet-18 by 1%. In addition, the performance of full-net in DDNN without EKD will be lower than the independently trained case because of sharing weights with “poor” sub-net models. After incorporating the EKD mechanism into DDNN, it can effectively ease the performance decline of full-net by transferring knowledge to sub-net models in each training step and full-net will gradually share weights from the “better” sub-net. In some cases, like “EKD-ResNet-50-41”,

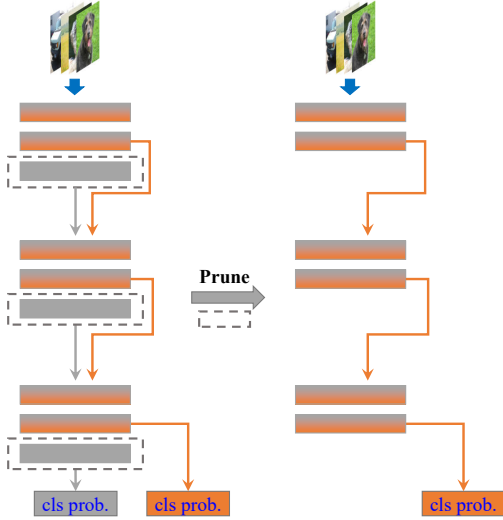


Fig. 4. DDNN with EKD training mechanism for depth-level pruning

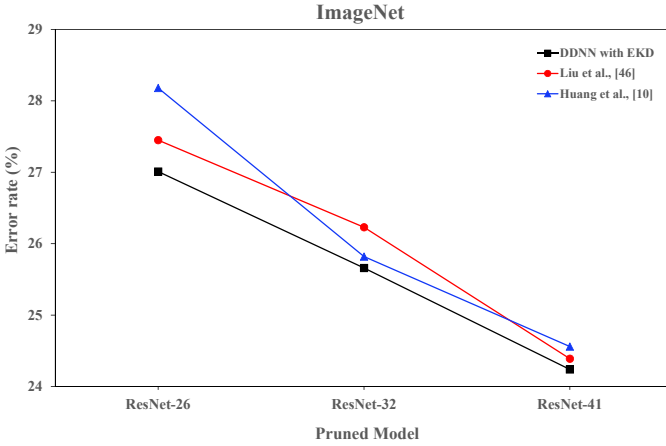


Fig. 5. Comparison with the depth-level pruning methods on ImageNet

the full-net even performs a little better than the independently trained model, which means the full-net model can also harvest considerable benefit from the “better” sub-net model.

3) *EKD for Network Pruning*: To obtain the small yet high-accuracy model, many network pruning methods generally compress the model via the redundant weights pruning or redundant layers removing. Nevertheless, these pruning methods usually involve a trained large model and a very costly training process including iterative pruning and fine-tuning after each pruning step, meanwhile, they can only harvest a high-accuracy small model once time.

From the network compression perspective, our DDNN with EKD training mechanism can also be used for the depth-level layers pruning task, and DDNN can simultaneously harvest multiple high-accuracy small models at one-time training. Once sub-nets in DDNN achieve very closed even better results than full-net, then we can directly prune the redundant layers of full-net without a fine-tuning process. The pruning method is showed in Fig. 4. To evaluate the effectiveness of this strategy, we make the comparison with recent notable depth-level pruning methods [10], [46] on the large-scale

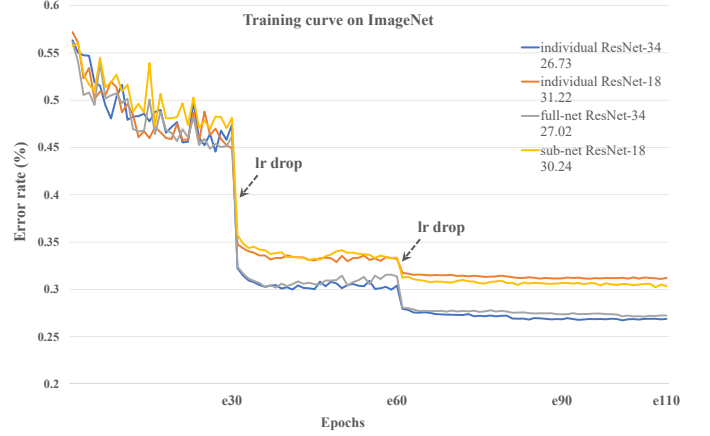


Fig. 6. Error rate (%) curves of EKD-ResNet-34-18 (full-net: ResNet-34 and sub-net: ResNet-18), individual ResNet-34, and individual ResNet-18 in training epoch.

ImageNet dataset. We both apply ResNet-50 as full-net (i.e., unpruned-net) for a fair comparison and obtain three small pruned-nets including ResNet-41, ResNet-32, and ResNet-26. Differently, we directly extract the pruned-net (i.e., sub-net) from DDNN trained with EKD mechanism, in contrast, they get the pruned-net by the costly trained process of depth-level pruning. Fig. 5 shows the competitive performance of our pruned sub-nets, where the lower error rate means better. From the results, we can see that our results (Black line in Fig. 5) surpass theirs on the three pruned-nets.

4) *Convergence Analysis*: Training our DDNN with EKD mechanism aims to optimize multi-objective functions from full-net and sub-nets. In Fig. 6, we select the DDNN of “EKD-ResNet-34-18” (i.e., full-net: ResNet-34 and sub-net: ResNet-18) on the ImageNet dataset as example to analysis the convergence of our proposed DDNN and individual ResNet-34/ResNet-18 trained with only the conventional hard labels. Firstly, the sub-net ResNet-18 in DDNN has a relatively large oscillation at the beginning of training, i.e., before the first learning rate (lr) dropping. This reason is that the sub-net in DDNN completely shares weight parameters with the full-net and it requires certain training epochs to adapt the multi-objective optimization. Secondly, the sub-net ResNet-18 and the full-net ResNet-34 in DDNN both converge smoothly after the second learning rate decay. Finally, the sub-net ResNet-18 in DDNN possesses an overall lower error rate than individual ResNet-18 after convergence. Meanwhile, the mean error rate gaps between of the sub-net ResNet-18/individual ResNet-18 and full net ResNet-34/individual ResNet-34 after epoch 60 are 0.61% and 0.39%, respectively. Compared with individual models, DDNN models of EKD training obtain higher accuracy of sub-net with the tiny performance sacrifice of full-net.

C. Ablation Study

In EKD mechanism, we mainly adopt the distillation on posterior class probabilities (KL loss) and self-attention on feature maps (MSE loss) to transfer knowledge from full-net to sub-nets. To respectively verify the effectiveness of each

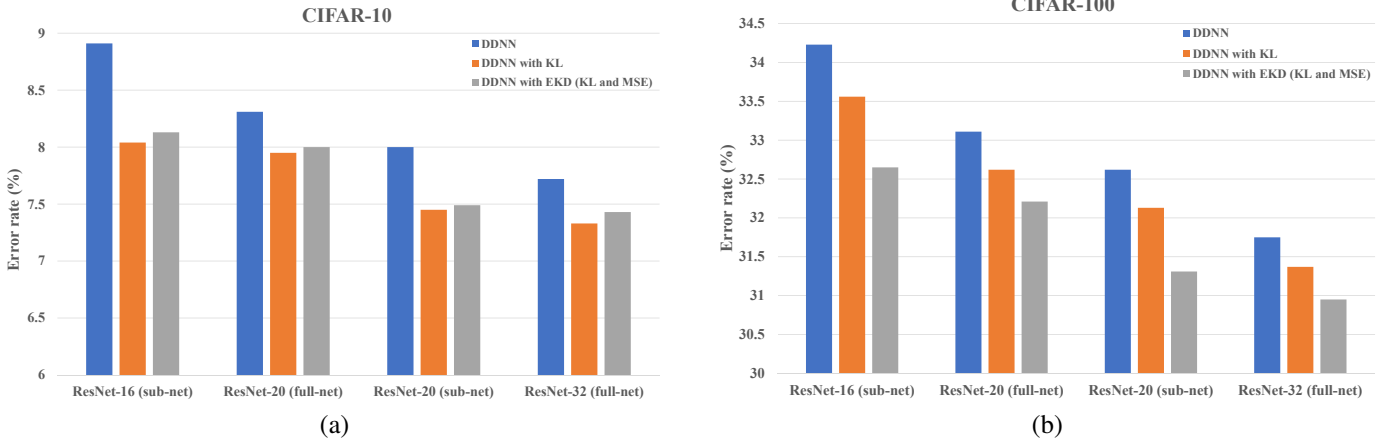


Fig. 7. Evaluate the influence of each component in EKD mechanism. We respectively take ResNet-20 and ResNet-32 as full-net. Sub-nets of them are ResNet-16 and ResNet-20 respectively. (a) Experiments on CIFAR-10; (b) Experiments on CIFAR-100.

component, we conduct exhaustive comparisons on the CIFAR dataset.

1) *Effectiveness of Distillation on Posterior Class Probability*: To evaluate the performance of posterior class probability distillation. We observe the effect of only applying the distillation KL loss to the optimization objective of DDNN. The related results are shown in Fig. 7, we can see that DDNN integrated the KL distillation (Orange) possesses a lower error rate than the DDNN with only hard labels (Blue), which effectively verifies the effectiveness of individual KL loss.

Besides, we also find that the DDNN with only KL distillation (Orange) even achieve a slightly better result than the DDNN with EKD (i.e., KL and MSE , Gray) from CIFAR-10 experiments in Fig. 7(a), which further demonstrates the effectiveness of KL posterior class probability distillation.

2) *Effectiveness of Self-attention on Feature Maps*: From CIFAR-100 experiments in Fig. 7(b), we can see that the DDNN with EKD training (KL and MSE , Gray) possesses obviously lower error rate than the DDNN with only KL distillation loss (Orange). It fully verifies the effectiveness of self-attention on feature maps, i.e., the self-attention module uses the MSE loss term to implement the knowledge transfer of feature level from full-net to sub-net, which can indeed improve the generalization of DDNN. Besides, we also conduct related experiments on the large-scale ImageNet dataset. Results display that the performance of DDNN can be improved further when we combine KL term and MSE term in EKD. This justifies that two components in EKD are also jointly effective.

Nevertheless, on CIFAR-10 experiments in Fig. 7(a), we also find that combining KL term and MSE term has slightly worse performance than individual KL , i.e., the KL and MSE in EKD maybe not jointly effective on a simple task. This is partly because the object recognition task of CIFAR-10 has only 10 classes which are relatively simple and our used deep ResNet architecture is enough complex to handle such a simple task. Thus, it may not requires the strong constraint of self-attention on feature maps of each stage to some extent. In contrast, this phenomenon is nonexistent on complex tasks,

TABLE IV
COMPARISON WITH TEACHER-TO-STUDENT METHODS ON IMAGENET

Method	Network	FLOPs	Params	Err. (%)
Teacher-to-Student [51]	ResNet-18 (teacher: ResNet-34)	1.8G	(11.7+21.8)M	30.2
DDNN with EKD	ResNet-18 (full-net: ResNet-34)	1.8G	21.8M	30.2
Teacher-to-Student [51]	ResNet-34 (teacher: ResNet-50)	3.6G	(21.8+25.6)M	26.1
DDNN with EKD	ResNet-32 (full-net: ResNet-50)	2.8G	25.6M	25.7

such as CIFAR-100 in Fig. 7(b) and large-scale ImageNet, i.e., combining KL term and MSE term has the obvious advantages than any individual one term for complex tasks.

3) *Comparison with Teacher-to-Student Mechanism*: In Fig. 1, we show the diagrams of the teacher-to-student mechanism and the proposed DDNN with EKD mechanism. Compared with the teacher-to-student paradigm, the proposed method has the following advantages: 1). **Flexibility**: Our constructed DDNN can dynamically extract different-depth sub-nets during the inference stage, in contrast, teacher-to-student can only provide one student model. 2). **Low-computation cost**: Our DDNN with EKD mechanism can be trained in an end-to-end manner, in contrast, the teacher-to-student paradigm has to first train a large teacher model and then train the student network with the extra supervised information from the trained teacher model.

Moreover, sub-nets in DDNN with EKD training can achieve comparative or even better results. Table IV gives the detailed comparisons (top-1 error rate %) of our proposed EKD mechanism and a notable teacher-to-student mechanism [51]. From the results, we can see that our sub-net ResNet-18 in DDNN (full-net: ResNet-34) with EKD training achieves similar performance as the teacher-to-student method. Note that we only need to train one full-net parameters (21.8M), in contrast, they require two network parameters of teacher and student. Especially, our sub-net ResNet-32 in DDNN with fewer parameters and FLOPs outperforms the student ResNet-34 model, which uses the same ResNet-50 as

full-net in DDNN and teacher model in teacher-to-student.

V. CONCLUSION

In this article, we propose the DDNN with only one full-net parameters to flexibly switch different-depth sub-nets or full-net according to the demand of different resource-limited devices. To improve the performance of sub-nets and full-net in DDNN, we further design the EKD training mechanism, which contains distillation on posterior class probabilities and self-attention on feature maps to exploit the potential representative capacity of the whole DDNN. Extensive experiments demonstrate that our DDNN with EKD training mechanism achieves competitive performance on multiple benchmark datasets. Also, sub-nets in DDNN with EKD training even obtain better results than recent notable pruned-nets. Compared with student networks trained with the teacher-to-student paradigm, our sub-nets with the same network architecture or even smaller network can also harvest similar or better performance. In the future, we will further enhance the understanding and applications of distillation and dynamic neural network by exploring more types of learning manners (e.g., adversarial learning, contrastive learning, and multi-view learning) for the training of DDNN.

REFERENCES

- [1] A. Krizhevsky, I. Sutskever, and G. E. Hinton, "ImageNet Classification with Deep Convolutional Neural Networks," in *Advances in Neural Information Processing Systems*, 2012, pp. 1106–1114.
- [2] K. He, X. Zhang, S. Ren, and J. Sun, "Deep residual learning for image recognition," in *IEEE Conference on Computer Vision and Pattern Recognition (CVPR)*, 2016, pp. 770–778.
- [3] R. B. Girshick, J. Donahue, T. Darrell, and J. Malik, "Rich Feature Hierarchies for Accurate Object Detection and Semantic Segmentation," in *IEEE Conference on Computer Vision and Pattern Recognition (CVPR)*, 2014, pp. 580–587.
- [4] K. He, X. Zhang, S. Ren, and J. Sun, "Spatial pyramid pooling in deep convolutional networks for visual recognition," *IEEE Transactions on Pattern Analysis and Machine Intelligence*, vol. 37, no. 9, pp. 1904–1916, 2015.
- [5] S. Ren, K. He, R. B. Girshick, and J. Sun, "Faster R-CNN: Towards Real-Time Object Detection with Region Proposal Networks," *IEEE Transactions on Pattern Analysis and Machine Intelligence*, vol. 39, no. 6, pp. 1137–1149, 2017.
- [6] E. Shelhamer, J. Long, and T. Darrell, "Fully convolutional networks for semantic segmentation," *IEEE Transactions on Pattern Analysis and Machine Intelligence*, vol. 39, no. 4, pp. 640–651, 2017.
- [7] G. Yang, X. Song, C. Huang, Z. Deng, J. Shi, and B. Zhou, "DrivingStereo: A large-scale dataset for stereo matching in autonomous driving scenarios," in *IEEE Conference on Computer Vision and Pattern Recognition (CVPR)*, 899–980 2019.
- [8] K. Simonyan and A. Zisserman, "Very deep convolutional networks for large-scale image recognition," in *International Conference on Learning Representations (ICLR)*, 2015.
- [9] G. Huang, Z. Liu, L. van der Maaten, and K. Q. Weinberger, "Densely Connected Convolutional Networks," in *IEEE Conference on Computer Vision and Pattern Recognition (CVPR)*, 2017, pp. 2261–2269.
- [10] Z. Huang and N. Wang, "Data-driven sparse structure selection for deep neural networks," in *European Conference on Computer Vision (ECCV)*, 2018, pp. 317–334.
- [11] Z. Wu, T. Nagarajan, A. Kumar, S. Rennie, L. S. Davis, K. Grauman, and R. S. Feris, "Blockdrop: Dynamic inference paths in residual networks," in *IEEE Conference on Computer Vision and Pattern Recognition (CVPR)*, 2018, pp. 8817–8826.
- [12] X. Wang, F. Yu, Z. Dou, T. Darrell, and J. E. Gonzalez, "Skipnet: Learning dynamic routing in convolutional networks," in *European Conference on Computer Vision (ECCV)*, 2018, pp. 420–436.
- [13] G. E. Hinton, O. Vinyals, and J. Dean, "Distilling the Knowledge in a Neural Network," in *arXiv:1503.02531*, 2015.
- [14] J. Ba and R. Caruana, "Do Deep Nets Really Need to be Deep?" in *Advances in Neural Information Processing Systems*, 2014, pp. 2654–2662.
- [15] A. Romero, N. Ballas, S. E. Kahou, A. Chassang, C. Gatta, and Y. Bengio, "Fitnets: Hints for thin deep nets," in *International Conference on Learning Representations (ICLR)*, 2015.
- [16] S. Zagoruyko and N. Komodakis, "Paying more attention to attention: Improving the performance of convolutional neural networks via attention transfer," in *International Conference on Learning Representations (ICLR)*, 2017.
- [17] A. Krizhevsky and G. E. Hinton, "Learning multiple layers of features from tiny images," Tech. Rep., 2009.
- [18] O. Russakovsky, J. Deng, H. Su, J. Krause, S. Satheesh, S. Ma, Z. Huang, A. Karpathy, A. Khosla, M. S. Bernstein, A. C. Berg, and F. Li, "Imagenet large scale visual recognition challenge," *International Journal of Computer Vision*, vol. 115, no. 3, pp. 211–252, 2015.
- [19] F. N. Iandola, M. W. Moskewicz, K. Ashraf, S. Han, W. J. Dally, and K. Keutzer, "SqueezeNet: AlexNet-level accuracy with 50x fewer parameters and <0.5MB model size," in *arXiv:1602.07360*, 2016.
- [20] C. Szegedy, S. Ioffe, V. Vanhoucke, and A. A. Alemi, "Inception-v4, Inception-ResNet and the Impact of Residual Connections on Learning," in *AAAI Conference on Artificial Intelligence*, 2017, pp. 4278–4284.
- [21] F. Chollet, "Xception: Deep Learning with Depthwise Separable Convolutions," in *IEEE Conference on Computer Vision and Pattern Recognition (CVPR)*, 2017, pp. 1800–1807.
- [22] C. Szegedy, V. Vanhoucke, S. Ioffe, J. Shlens, and Z. Wojna, "Rethinking the Inception Architecture for Computer Vision," in *IEEE Conference on Computer Vision and Pattern Recognition (CVPR)*, 2016, pp. 2818–2826.
- [23] A. G. Howard, M. Zhu, B. Chen, D. Kalenichenko, W. Wang, T. Weyand, M. Andreetto, and H. Adam, "Mobilenets: Efficient convolutional neural networks for mobile vision applications," in *arXiv:1704.04861*, 2017.
- [24] X. Zhang, X. Zhou, M. Lin, and J. Sun, "Shufflenet: An extremely efficient convolutional neural network for mobile devices," in *IEEE Conference on Computer Vision and Pattern Recognition (CVPR)*, 2018, pp. 6848–6856.
- [25] I. Hubara, M. Courbariaux, D. Soudry, R. El-Yaniv, and Y. Bengio, "Binarized neural networks," in *Advances in Neural Information Processing Systems*, 2016, pp. 4107–4115.
- [26] M. Rastegari, V. Ordonez, J. Redmon, and A. Farhadi, "Xnor-net: Imagenet classification using binary convolutional neural networks," in *European Conference on Computer Vision (ECCV)*, 2016, pp. 525–542.
- [27] H. Li, S. De, Z. Xu, C. Studer, H. Samet, and T. Goldstein, "Training quantized nets: A deeper understanding," in *Advances in Neural Information Processing Systems*, 2017, pp. 5811–5821.
- [28] S. Han, H. Mao, and W. J. Dally, "Deep compression: Compressing deep neural network with pruning, trained quantization and Huffman coding," in *International Conference on Learning Representations (ICLR)*, 2016.
- [29] M. Courbariaux, Y. Bengio, and J.-P. David, "BinaryConnect: Training Deep Neural Networks with binary weights during propagations," in *Advances in Neural Information Processing Systems*, 2015, pp. 3123–3131.
- [30] S. Han, J. Pool, J. Tran, and W. J. Dally, "Learning both Weights and Connections for Efficient Neural Network," in *Advances in Neural Information Processing Systems*, 2015, pp. 1135–1143.
- [31] S. Han, H. Mao, and W. J. Dally, "Deep Compression: Compressing Deep Neural Network with Pruning, Trained Quantization and Huffman Coding," in *International Conference on Learning Representations (ICLR)*, 2016.
- [32] Y. Guo, A. Yao, and Y. Chen, "Dynamic Network Surgery for Efficient DNNs," in *Advances in Neural Information Processing Systems*, 2016, pp. 1379–1387.
- [33] S. Anwar, K. Hwang, and W. Sung, "Structured pruning of deep convolutional neural networks," *ACM J. Emerg. Technol. Comput. Syst.*, vol. 13, no. 3, pp. 32:1–32:18, 2017.
- [34] H. Li, A. Kadav, I. Durdanovic, H. Samet, and H. P. Graf, "Pruning filters for efficient convnets," in *International Conference on Learning Representations (ICLR)*, 2017.
- [35] P. Molchanov, S. Tyree, T. Karras, T. Aila, and J. Kautz, "Pruning convolutional neural networks for resource efficient inference," in *International Conference on Learning Representations (ICLR)*, 2017.
- [36] G. Urban, K. J. Geras, S. E. Kahou, Ö. Aslan, S. Wang, A. Mohamed, M. Philipose, M. Richardson, and R. Caruana, "Do deep convolutional nets really need to be deep and convolutional?" in *International Conference on Learning Representations (ICLR)*, 2017.

- [37] G. Chen, W. Choi, X. Yu, T. X. Han, and M. Chandraker, "Learning efficient object detection models with knowledge distillation," in *Advances in Neural Information Processing Systems*, I. Guyon, U. von Luxburg, S. Bengio, H. M. Wallach, R. Fergus, S. V. N. Vishwanathan, and R. Garnett, Eds., 2017, pp. 742–751.
- [38] Q. Li, S. Jin, and J. Yan, "Mimicking very efficient network for object detection," in *IEEE Conference on Computer Vision and Pattern Recognition (CVPR)*, 2017, pp. 7341–7349.
- [39] J. Xie, B. Shuai, J. Hu, J. Lin, and W. Zheng, "Improving fast segmentation with teacher-student learning," in *British Machine Vision Conference (BMVC)*, 2018, p. 205.
- [40] Y. Liu, K. Chen, C. Liu, Z. Qin, Z. Luo, and J. Wang, "Structured knowledge distillation for semantic segmentation," in *IEEE Conference on Computer Vision and Pattern Recognition (CVPR)*, 2019, pp. 2604–2613.
- [41] Y. Chen, N. Wang, and Z. Zhang, "Darkrank: Accelerating deep metric learning via cross sample similarities transfer," in *Proceedings of the Thirty-Second AAAI Conference on Artificial Intelligence*, S. A. McIlraith and K. Q. Weinberger, Eds. AAAI Press, 2018, pp. 2852–2859.
- [42] L. Liu and J. Deng, "Dynamic deep neural networks: Optimizing accuracy-efficiency trade-offs by selective execution," in *AAAI Conference on Artificial Intelligence*, 2018, pp. 3675–3682.
- [43] G. Huang, D. Chen, T. Li, F. Wu, L. van der Maaten, and K. Q. Weinberger, "Multi-scale dense networks for resource efficient image classification," in *International Conference on Learning Representations (ICLR)*, 2018.
- [44] J. Yu, L. Yang, N. Xu, J. Yang, and T. S. Huang, "Slimmable neural networks," in *International Conference on Learning Representations (ICLR)*, 2019.
- [45] J. Yu and T. S. Huang, "Universally slimmable networks and improved training techniques," in *IEEE International Conference on Computer Vision (ICCV)*. IEEE, 2019, pp. 1803–1811.
- [46] Z. Liu, M. Sun, T. Zhou, G. Huang, and T. Darrell, "Rethinking the value of network pruning," in *International Conference on Learning Representations (ICLR)*, 2019.
- [47] A. Paszke, S. Gross, F. Massa, A. Lerer, J. Bradbury, G. Chanan, T. Killeen, Z. Lin, N. Gimelshein, L. Antiga, A. Desmaison, A. Köpf, E. Yang, Z. DeVito, M. Raison, A. Tejani, S. Chilamkurthy, B. Steiner, L. Fang, J. Bai, and S. Chintala, "Pytorch: An imperative style, high-performance deep learning library," in *Advances in Neural Information Processing Systems*, 2019, pp. 8024–8035.
- [48] C. Szegedy, W. Liu, Y. Jia, P. Sermanet, S. E. Reed, D. Anguelov, D. Erhan, V. Vanhoucke, and A. Rabinovich, "Going deeper with convolutions," in *IEEE Conference on Computer Vision and Pattern Recognition (CVPR)*, 2015, pp. 1–9.
- [49] K. He, X. Zhang, S. Ren, and J. Sun, "Identity mappings in deep residual networks," in *European Conference on Computer Vision (ECCV)*, 2016, pp. 630–645.
- [50] Z. Liu, J. Li, Z. Shen, G. Huang, S. Yan, and C. Zhang, "Learning efficient convolutional networks through network slimming," in *IEEE International Conference on Computer Vision (ICCV)*, 2017, pp. 2755–2763.
- [51] A. K. Mishra and D. Marr, "Apprentice: Using knowledge distillation techniques to improve low-precision network accuracy," in *International Conference on Learning Representations (ICLR)*, 2018.



Shuchang Lyu received the B.S. degree in communication and information from Shanghai University, Shanghai, China, in 2016, and the M.E. degree in communication and information system from the School of Electronic and Information Engineering, Beihang University, Beijing, China, in 2019.

He is currently pursuing the Ph.D. degree with the School of Electronic and Information Engineering, Beihang University, Beijing. His research interests include deep learning, pattern recognition, image classification, one-shot semantic segmentation and

object detection.



Ting-Bing Xu received the B.S. degree in automation from the China University of Petroleum, Qingdao, China, in 2014, and the Ph.D. degree in computer applied technology from the National Laboratory of Pattern Recognition (NLPR), Institute of Automation of Chinese Academy of Sciences, Beijing, China, in 2020.

He was a Visiting Researcher with the Department of Computer Science and Intelligent Systems, Osaka Prefecture University, Osaka, Japan, in 2018. He is currently a Postdoctoral Fellow with the School of Instrumentation Science and Opto-electronics Engineering, Beihang University, Beijing. His research interests include deep learning, machine learning, pattern recognition, handwriting recognition, and machine vision.



Guangliang Cheng received the B.S. degree in automation from the China University of Petroleum, Qingdao, China, in 2012, and the Ph.D. degree in pattern recognition and intelligence systems from the Institute of Automation of Chinese Academy of Sciences, Beijing, China, in 2017.

He was a Postdoctoral Fellow with the Institute of Remote Sensing and Digital Earth, Chinese Academy of Sciences, Beijing, China, from 2017 to 2019. He is currently a Senior Research Manager with the SenseTime Research, Beijing. His research interests include autonomous driving, scene understanding, pattern recognition, machine learning, and remote sensing image processing.